Electrochemical and Spectroscopic Investigations of the Cytochrome bc_1 Complex from *Rhodobacter capsulatus*[†]

F. Baymann,*[,‡] D. E. Robertson,[§,||] P. L. Dutton,[§] and W. Mäntele[⊥]

Institute de Biologie Physico-chimique, 13, rue Pierre et Marie Curie, 75005 Paris, France, Johnson Research Foundation, Department of Biochemistry and Biophysics, University of Pennsylvania, Philadelphia, Pennsylvania 19104, and Institut für Biophysik, Johann Wolfgang von Goethe Universität, Theordor-Stem-Kai 7, 60540 Frankfurt/Main, Germany

Received March 11, 1999; Revised Manuscript Received June 16, 1999

ABSTRACT: The cytochrome bc_1 complex from *Rhodobacter capsulatus* was investigated by protein electrochemistry and visible/IR spectroscopy. Infrared difference spectra, which represent redox-induced conformational changes of cofactors and their protein environments, show signals of the hemes, the quinone Q_i, and small conformational changes of the protein backbone. Furthermore, band features were tentatively assigned to protonated aspartic or glutamic acids involved in the redox transition of each of the *b* hemes, a proline in that of the [2Fe-2S] protein, and an arginine in that of cytochrome b_H. The midpoint potential of the [2Fe-2S] protein was determined for the first time at physiological temperature to be +290 mV at pH 8.7. The reduced minus oxidized difference extinction coefficients of the α-bands of the cytochromes were calculated as 11.5, 19, and 6.7 mM^{-1} cm^{-1} for cytochromes c_1, b_H, and b_L, respectively. A novel method has been developed to quantify protonation reactions of the complex during the redox reactions of its cofactors by evaluation of the buffer signals in the midinfrared region. Values will be discussed in relation to the pH dependence of the midpoint potentials.

Cytochrome bc_1 complexes are transmembrane proteins working as proton pumps in photosynthesis of green plants, algae, heliobacteria, and cyanobacteria and in respiration of eukaryotes and prokaryotes. They are formed by a minimum of three subunits: one contains a *c*-type heme (cytochrome c_1 or cytochrome *f*), one holds a [2Fe-2S] cluster of the Rieske type, and the third one contains two *b*-hemes (cytochrome b_H and cytochrome b_L). The cytochrome bc_1 complex of *Rhodobacter capsulatus* does not contain any additional subunits. The complex has two quinone-binding sites: a quinol-oxidizing site close to the [2Fe-2S] cluster and the heme b_L is named the Q_o site. A quinone-reducing site (Q_i) is close to the heme b_H on the other site of the membrane. Compared with the quinone of the membrane pool and the Q_o site, the Q_i site stabilizes the semiquinone form.

The structure of the bc_1 complex has been elucidated by biochemical, biophysical, and molecular biology studies (*1*−*14*). Recently, a crystal structure has been published for the bc_1 complex from bovine heart, chicken, and rabbit mitochondria (*15*, *16*). The complex crystallizes as a dimer. The location and amino acid composition of the quinone-binding sites has been well characterized, in particular by studying the resistance of mutants of the complex against inhibitors that block specifically one of these binding sites (see refs *11* and *17* for reviews) and recently by the structure of the complex in the presence of different inhibitors (*16*).

For the cotransfer of protons and electrons the Q-cycle model has been proposed (*6*, *14*, *18*, *19*): one of the electrons of the quinol, which becomes oxidized at the Q_o site, subsequently reduces the [2Fe-2S] cluster and cytochrome c_1. The second electron is transferred across the membrane by the *b* hemes to reduce finally a quinone bound to the Q_i site.

The midpoint potentials for the cytochrome bc_1 complex of *Rb. capsulatus* at pH 7 are reported to be −89 mV[1] for cytochrome b_L, +40 mV for cytochrome b_H, +290 mV for cytochrome c_1 and +274 mV for the [2Fe-2S] cluster (*20*).

In the present work a combination of protein electrochemistry and spectroscopy (*21*) has been used to determine the midpoint potentials of the cofactors and the redox-induced difference spectra of each compound of the complex in the visible (vis) and midinfrared spectral region. Difference spectra in the midinfrared spectral region indicate conformational changes of the backbone and the side chains, protonation and deprotonation reactions of amino acid residues, hydrogen-bonding changes to side chains and to the backbone, and interactions between prosthetic groups and the protein. The infrared (IR) difference signals can therefore lead to information about the molecular mechanism of the complex. Protonation reactions of the buffer, which occur by proton release from the complex, lead to IR difference signals as well. They have been quantified by a novel method developed in the framework of this study to determine the number of protons involved in the redox reaction of each cofactor.

[†] F.B. is supported by E.C. Fellowship ERBFMBICT960707 and P.L.D. by U.S. Public Health Service Grant GM-27309.

* To whom correspondence should be addressed: Phone 0033 1 43 25 26 09; FAX 0033 1 40 46 83 31; email baymann@ibpc.fr.

[‡] Institute de Biologie Physico-chimique.

[§] University of Pennsylvania.

[||] Present address: Diversa, 10665 Sorrento Valley Rd., San Diego, CA 92121.

[⊥] Johann Wolfgang von Goethe Universität.

[1] All redox potentials are given with respect to the standard hydrogen electrode.

10.1021/bi990565b CCC: $18.00 © 1999 American Chemical Society
Published on Web 09/17/1999

MATERIALS AND METHODS

Protein Preparation. The cytochrome bc_1 complex from *Rb. capsulatus* was prepared according to the method described in Ljungdahl et al. (*22*) and Robertson et al. (*20*). The preparation was done from the mutant strain pMTO-404/MT-RKB1, a bc_1 overproducer. The complex was solubilized in the detergent dodecyl maltoside and has an activity close to *in vivo* level (*20*). The purified complex was transferred to either 100 mM Tris-HCl buffer at pH 8.7 or 100 mM potassium phosphate buffer at pH 6.5 by dialysis. Both buffers contained 0.1 mg/mL dodecyl maltoside and 50 mM KCl as a conducting salt for the electrochemical experiments and were used throughout this work. The protein solution was subsequently concentrated by ultracentrifugation (44000*g*). For storage and transport this solution was frozen. Before every experiment an aliquot was thawed and further concentrated in Microcon ultrafiltration cells (Amicon, Denver, MA) to a final concentration of 1−5 mM (determined from the difference spectra as described below). To obtain the ^{15}N-labeled complex, bacteria were grown in ^{15}N medium and the complex was prepared as described above.

The replacement of exchangeable hydrogen atoms in the complex with deuterium was done by microdialysis in ^2H_2O buffer of identical composition.

Sample Preparation. Aliquots (6 μL) of the concentrated protein solution were used to fill the IR-transparent thin-layer electrochemical cell described previously (*21*, *23*). The average protein concentration was 2 mM. The path length of the cell can range between 4 and 12 μm and thus was determined for every experiment. The gold grid used as the working electrode was modified with pyridine-3-carboxyaldehyde thiosemicarbazone (PATS-3) as described in Baymann et al. (*23*) to avoid irreversible protein adhesion. A mixture of 11 different mediators (Table 1) was added to the solution of cytochrome bc_1 complex in order to ensure and to accelerate the equilibration of the cofactors with the applied potential. Each of the mediators was used at a concentration of 40 μM, i.e., 50-fold less concentrated than the average protein concentration.

Control measurements with the protein without mediators and with mediators in the absence of the protein were performed in order to test whether direct reactions of the cofactors at the modified gold electrode takes place and to verify that no spectral changes from the mediators are present in the IR difference spectra of the protein.

Table 1: Mediator Mixture for Electrochemical Experiments[a]

mediator	midpoint potential (mV)	soluble in
1,1′-ferrocenedicarbonic acid	+644	
ferricyanide	+430	water
1,1′-dimethylferrocene	+341	ethanol
tetrachlorobenzoquinone	+280	ethanol
ruthenium hexamine chloride	+200	water
1,2-naphthoquinone	+140	ethanol
N-methylphenazonium methylsulfate	+55	ethanol
N-ethylphenazonium ethylsulfate	+45	ethanol
menadione	−12	ethanol
2′-(OH)-1,4-naphthoquinone	−125	water
anthraquinone-2-sulfonate	−225	water
benzylviologen	−352	water

[a] Mediator mixture used in the electrochemical cell to equilibrate the applied potential with the cofactors. Mediators were used at a concentration of 40 μM. The midpoint potentials are given for pH 7.

Spectroscopy and Electrochemistry. The electrochemical cell was thermostated at 278 K and connected to a potentiostat, constructed in the laboratory. Infrared spectra were recorded on a Bruker IFS 25 Fourier transform infrared (FTIR) spectrophotometer. A combined visible/IR setup was used to allow simultaneous measurements of spectra in the IR and visible range.

Potentials as indicated in Table 2 were applied to the complex and equilibration between the cofactors and the electrode was followed by the spectral changes in the visible range. Complete equilibrium was reached in 1−40 min with cytochrome c_1 having the fastest and cytochrome b_L the slowest reaction kinetics. After equilibration, spectra were recorded from 400 to 700 nm in the visible and from 1800 to 1000 cm^{-1} in the midinfrared spectral region. Typically, 128 interferrograms at 4 cm^{-1} resolution were coadded for each single-beam IR spectrum and transformed using triangular apodization. If necessary, difference spectra from several redox reactions were averaged to improve the signal-to-noise ratio.

In order to attribute the difference signals in the spectra to the redox transition of a specific cofactor, redox titrations of the visible and IR difference spectra were performed. Selected potentials were applied in steps of 30 mV and equilibration times of 2−10 min were used. The reference potential was +450 mV for the titration of cytochrome c_1 and the [2Fe-2S] protein and +240 mV for cytochrome b_H and the quinone Q_i. The final potentials were +210 and −90 mV, respectively. After each 30 mV changes in applied potential, the reference potential was applied again, thus minimizing baseline drifts. Each redox titration was done in reductive and oxidative directions.

At pH 6.5 the midpoint potentials of the [2Fe-2S] protein and of cytochrome c_1 are too close to separate their respective redox difference spectra in a titration. At pH 8.7 the midpoint potential of the [2Fe-2S] protein is shifted and the midpoint potentials of cytochrome c_1 and the [2Fe-2S] protein are separated by approximately 60 mV. The spectra of the [2Fe-2S] protein were thus calculated by a weighted subtraction of the spectra obtained in the potential range where predominantly cytochrome c_1 undergoes its redox reaction (+450 to +300 mV) from those spectra obtained in a second potential range (+300 to +200 mV), where mainly redox reactions of the [2Fe-2S] protein are induced. The weighting factor was determined from the amplitude of the α-band of cytochrome c_1 as measured simultaneously at the same sample in the visible spectral region.

With all samples, a redox titration of the spectra in the visible range was performed between +460 and −290 mV either reductively or oxidatively or both. The evaluation of these data resulted in the midpoint potentials and extinction coefficients of the cytochromes of the complex.

Calculation Procedures. The data of redox titrations were transmitted to the global fit program ME_h-fit (*24*) in order to calculate the midpoint potential and the difference spectra for every redox component participating in the overall redox reaction. Introduction of weights for every amplitude, calculated from standard deviations of multiple baselines, allowed us to minimize the influence of spectral regions with higher noise level.

Protonation Reactions. The pH-dependent buffer signals of Tris-HCl and potassium phosphate buffer were used to calibrate the number of protons released from the complex during the reduction of its cofactors. Tris-HCl and potassium phosphate buffer both absorb only in the 1200−1000 cm^{-1} spectral region, where no protein absorption of significant amplitude is expected. Extinction coefficients of the buffer difference signals were calculated from the difference of absorbance spectra of the buffers as obtained at pH 6 and pH 7 for potassium phosphate buffer and at pH 8 and pH 9 for Tris-HCl buffer. We determined an extinction coefficient $\Delta\epsilon_{1086-1020cm^{-1}}$ of 0.79 mM^{-1} cm^{-1} for potassium phosphate buffer. The maximum at 1086 cm^{-1} corresponds to the antisymmetric stretch vibration of the HPO_4^{2-} group, which appears in the difference spectra due to the deprotonation of the buffer system. Proton release from Tris-HCl buffer causes a minimum at 1066 cm^{-1} (C−N vibration from the CNH_3^+ group). A $\Delta\epsilon_{1066-1102cm^{-1}}$ of 0.27 mM^{-1} cm^{-1} was determined for this signal. The reference wavelengths at 1020 and 1102 cm^{-1} for potassium phosphate and Tris-HCl buffer, respectively, were chosen at positions of isosbestic points in the difference spectra of the two buffer systems (spectra not shown).

The number of protons released by the protein during the oxidation of a cofactor was then calculated from the amplitude of the buffer signal in the respective redox-induced difference spectra of the protein sample. For this procedure the path length of the sample and the protein concentration has to be known. The path length was determined in each experiment from the amplitude of the water mode at 2132 cm^{-1} in the absorbance spectra of the sample. To calibrate this mode, an absorbance spectrum from a sample in a cuvette with a fixed path length of 13 μm was used. The concentration of the reacting protein was determined from the α-band absorption of the cytochromes and their respective extinction coefficients, determined in this work.

RESULTS

Reactions of the Cofactors of Cytochrome bc_1 Complex at the Modified Gold Electrode. Cytochrome c_1 reacts directly, i.e., in the absence of mediators, at the modified gold electrode. The [2Fe-2S] protein and cytochrome b_H both show direct reactions at pH 6.5, but at pH 8.7 they need redox mediators to exhibit reversible redox reactions. Q_i reacts at pH 8.7 only in the presence of mediators. At pH 6.5, slow reactions in the absence of mediators could be observed. Cytochrome b_L reacts only if mediators are present at either pH value. The presence of benzylviologen in the mediator mixture has been proven to considerably accelerate the redox reactions of cytochrome b_L in the electrochemical cell (David Kramer, personal communication). Reactions of quinone bound to the Q_o binding site were not observed in this work.

Difference Spectra and Extinction Coefficients of the Cytochromes in the Visible Spectral Range. Figure 1 shows the difference spectra of the cytochromes from the bc_1 complex as calculated from redox titrations. Normalization was done, assuming a reduced minus oxidized difference extinction coefficient of 28.5 mM^{-1} cm^{-1} for the absorption of the two *b*-hemes at 563 nm as used by Yu et al. (*25*). This value corresponds to the one determined by Iba et al. (*26*) to 28.3 mM^{-1} cm^{-1}. Cytochrome b_L has a split α-band, which peaks at 566 and 558 nm. The overall half-width is 17.5 nm and the difference extinction coefficient at 566 nm − 575 nm is 6.7 mM^{-1} cm^{-1}. The α-band of cytochrome b_H has a half-width of 9 nm, a difference extinction coefficient of 21.9 mM^{-1} cm^{-1} at 561 nm − 575 nm, and shows a small shoulder at 558 nm. The spectrum of cytochrome c_1 has its α-band maximum at 553 nm with a half width of 6 nm. The difference extinction coefficient at 553 nm − 575 nm was determined to 11.9 mM^{-1} cm^{-1}. The difference spectrum shows an additional negative signal around 690 nm (data not shown). This signal of small amplitude is very broad and reaches its maximum amplitude in a reductive redox titration at +230 mV, indicating that it is caused by reduction of cytochrome c_1.

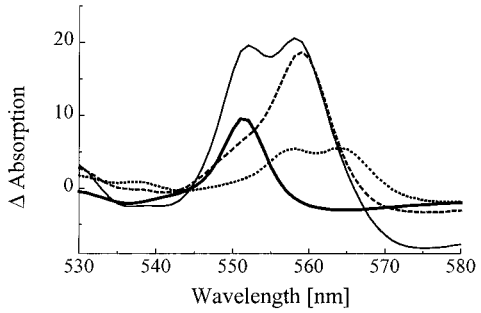

FIGURE 1: Difference spectra in the visible range of the cytochromes of cytochrome bc_1 complex from *Rb. capsulatus* as calculated from a redox titration (−310 to +460 mV) at pH 6.5. Spectra were normalized to a protein concentration of 1 mM and a path length of 1 cm. Cytochrome c_1, bold line; cytochrome b_H, dashed line; cytochrome b_L, dotted line; total cytochrome bc_1 complex, thin line.

Midpoint Potentials of the Cofactors of Cytochrome bc_1 Complex. The redox midpoint potentials of the hemes of cytochrome bc_1 *complex* are shown in Table 2. The equilibration between the cofactors and the applied potential was achieved in all titrations for each of the cofactors except for cytochrome b_L, for which the equilibrium could be reached only in a single titration at each pH value. For the other titrations, the "true" midpoint potential was assumed to be the average value of midpoint potentials determined for the titration in oxidative and reductive steps. At pH 8.7 a semiquinone anion is stabilized in part of the Q_i binding sites (*12*). Its presence shifts the redox potential of cytochrome b_H to +90 mV at pH 8.7. Despite the shift of the redox potential of the population, changes in the corresponding visible difference spectra could not be detected. The respective amplitudes of the difference spectra of the two populations of cytochrome b_H always add up to the same amplitude observed for cytochrome b_H at pH 6.5, where only the low-potential form is present.

The [2Fe-2S] protein and the quinones have only very small extinction coefficients in the visible spectral range. They are not detectable if cytochromes with high extinction coefficients in the respective spectral regions are present in the same sample. Therefore redox titrations of the IR difference spectra were performed in this work in order to determine the redox potentials of the [2Fe-2S] protein and of Q_i. For both cofactors a reductive and an oxidative IR titration at pH 6.5 and pH 8.7 was done. Midpoint potentials were determined to be +337 mV (pH 6.5) and +288 mV (pH 8.7) for the [2Fe-2S] protein and +170 mV (pH 6.5) and

Table 2: Midpoint Potentials of the Cofactors of bc_1 Complex[a]

	experimental values of this work		literature values		
compound	pH 6.5	pH 8.7	pH 6.5	pH 7	pH 8.7
cytochrome c_1	+354 ± 21	+335 ± 25		+290	
[2Fe-2S] protein	+337	+288	+310	+274 to +308	+240
cytochrome b_H	+72 ± 21	−11 ± 36		+40	
quinone Q_i	+170	+44	+180		+48
cytochrome b_L	−86 ± 28	−145 ± 52		−90	
cytochrome b_{150}		+91 ± 32			≈+120[b]

[a] Midpoint potentials of the cofactors were determined from electrochemical redox titrations by a global fit procedure. Average values and standard deviations from 16 redox titrations in the visible range at pH 8.7 and 19 at pH 6.5 are given in millivolts (potential range +510 to −240 mV). Values for the [2Fe-2S] protein and the quinone Q_i were determined from one IR redox titration each (potential range +450 to +200 mV for the [2Fe-2S] protein and +240 to −90 mV for the quinone Q_i). Literature values (*4*, *6*, *12*, *20*, *28*, *29*, *43*, *44*, *58*) are given for comparison. [b] pH 8.45.

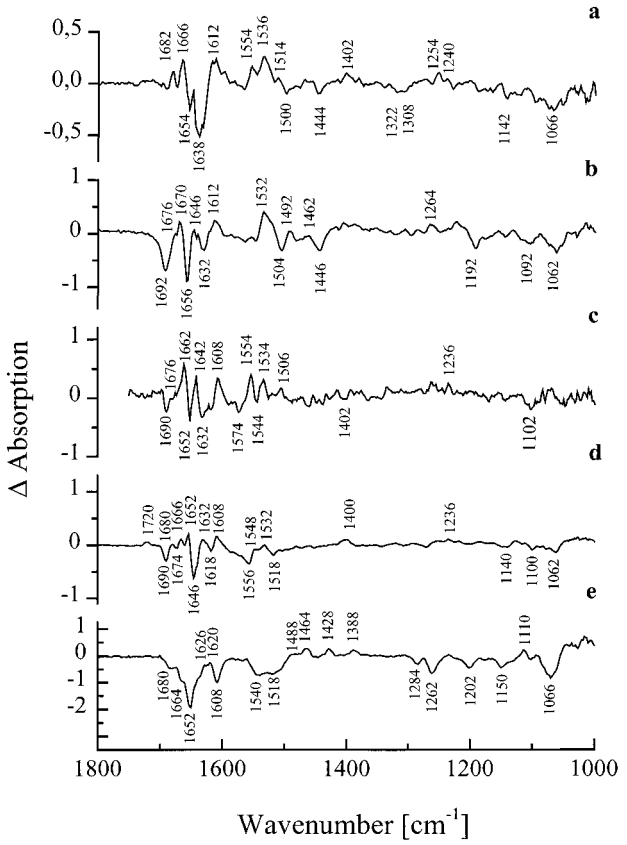

FIGURE 2: Reduced minus oxidized IR difference spectra of the compounds of cytochrome bc_1 complex from *Rb. capsulatus* obtained in Tris-HCl buffer at pH 8.7, normalized to a protein concentration of 1 mM and a path length of 1 cm. (a) Cytochrome c_1, (b) [2Fe-2S] protein, (c) cytochrome b_H, (d) cytochrome b_L, and (e) quinone bound to Q_i binding site. For experimental details see text.

+44 mV (pH 8.7) for Q_i. These values are comparable to literature values obtained by electron paramagnetic resonance (EPR) redox titrations (*4*, *6*, *12*, *20*, *27*−*29*).

IR Difference Spectra. The redox-induced infrared difference spectra of the cofactors of cytochrome bc_1 complex are shown in Figure 2 for spectra obtained at pH 8.7 and in Figure 3 for pH 6.5. The IR difference spectra of cytochrome c_1 and the [2Fe-2S] protein and of cytochrome b_H and the quinone Q_i each were calculated from a redox titration in the IR range. At pH 6.5 the [2Fe-2S] protein and cytochrome c_1 have similar redox potentials. A separation of their respective amplitudes is thus not possible. The difference spectrum originating from the redox reactions of both

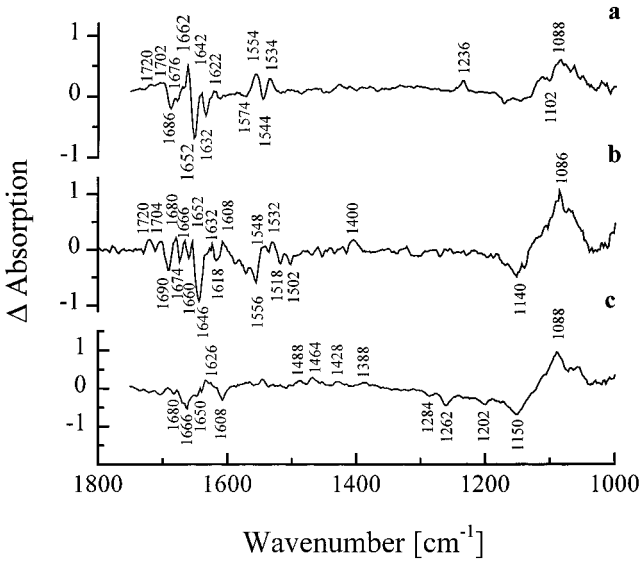

FIGURE 3: Reduced minus oxidized IR difference spectra of the compounds of cytochrome bc_1 complex from *Rb. capsulatus* obtained in potassium phosphate buffer at pH 6.5, normalized to a protein concentration of 1 mM and a path length of 1 cm. (a) Cytochrome b_H, (b) cytochrome b_L, and (c) quinone bound to Q_i binding site. For experimental details see text.

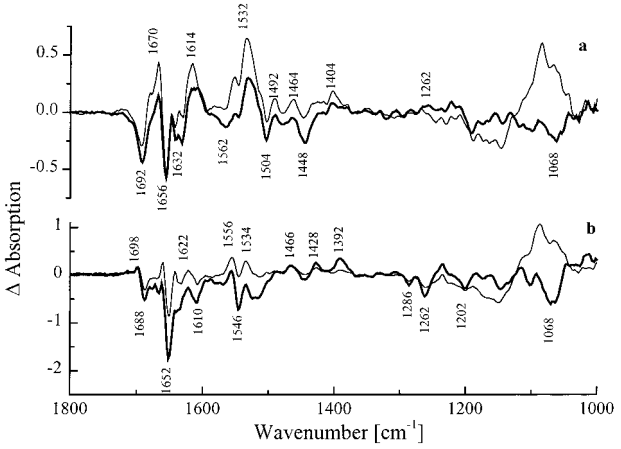

FIGURE 4: Reduced minus oxidized infrared difference spectra of (a) cytochrome c_1 and the [2Fe-2S] protein and (b) cytochrome b_H and the quinone bound to the Q_i binding site. Measurements were done in Tris-HCl buffer at pH 8.7 (bold lines) and in potassium phosphate buffer at pH 6.5 (thin lines). Spectra were normalized to a protein concentration of 1 mM and a path length of 1 cm.

cofactors is shown in Figure 4a as obtained at pH 6.5 and pH 8.7. Figure 4b shows the difference spectrum of the redox

Table 3: Peak Position and Band Assignment in IR Difference Spectra[a]

cytochrome c_1	[2Fe-2S] protein	cytochrome b_H	cytochrome b_L	quinone Q_i	assignment
		1720(+), 1702(+)	*1720(+), 1704(+)*		−C═O Asp/Glu
1682(+), 1654(−), 1666(+), 1638(−), 1612(+)	1692(−), 1676(+), 1670(+), 1656(−), 1646(+), 1632(−), 1612(+)	***1690(−)***, *1686(−)*, 1676(+), 1662(+), 1652(−), 1642(+), 1632(−), *1622(+)*	1690(−), 1680(+), 1674(−), 1666(+), 1660(−), 1652(+), 1646(−), 1632(+), 1618(−)	1680(−), ***1652(−)***, *1642(+)*, 1626(+), 1620(+)	amide I
		1676(+), *1634(+)*, *1622(+)*			$CN_3H_5^{s,as}$ Arg
				1666(−), 1650(−)	$C{=}O^{s}$ quinone
		1642(+)			$CN_3H_5^{s,sym}$ Arg
				1608(−)	$C{=}C^{s}$ quinone ring
		1608(+)	1608(+)		CαCβ heme vinyl
		1574(−)			$COO^{-s,as}$ Asp,Glu
1554(+)		1554(+)	1548(+)		C*a*C*m* heme
1536(+)		1534(+)	1532(+)		C*b*C*b* heme
1514(+), 1500(−)	1532(+), 1504(−), 1492(+)	1574(−), 1544(−)	1556(−)	***1540(−)***, ***1518(−)***	amide II
				1488(+)	C−C semiquinone ring
				1464(+)	$C{-}CH_2$ isoprenoid or methyl/methoxy group of quinone
				1428(+)	C−C, quinol
	1462(+), 1446(+)				ring vibration Pro/Trp
		1402(−)			$COO^{-s,sym}$ Asp,Glu
1402(+)			1400(+)		C*a*N heme
				1388(+)	$C{-}CH_3$ isoprenoide
				1284(−)	C−C quinone
				1262(−)	C−O or C−C quinone
1240(+)		1236(+)	***1236(+)***		C*m*H heme
				1202(−), 1150(−)	methoxy grp. quinone
			1140(−)		CαCβ^{s} heme vinyl
		1102(−)	***1100(−)***		$=CH_2^{d}$ heme vinyl
1066(−)	***1062(−)***		***1062(−)***	***1066(−)***	Tris-HCl buffer
	1084(+)	*1088(+)*	*1086(+)*	*1088(+)*	*phosphate buffer*

[a] Peak positions of the reduced minus oxidized difference signals in the IR difference spectra; preliminary band assignments to the absorption of protein and cofactor bands are given. (−) Signal is a minimum; (+) signal is a maximum; italic type indicates signals that are only present in the spectra obtained at pH 6.5 (Figure 3); boldface italic type indicates signals only present at pH 8.7 (Figure 2); underlined entries indicate shifts of band positions assigned in the text due to $^1H/^2H$ exchange (except the amide I signals, all shifted by a few wavenumbers); boldface type indicates interpreted shifts due to ^{15}N isotope labeling.

reactions of both cytochrome b_H and the quinone bound to Q_i binding site. Data were normalized to a protein concentration of 1 mM and a path length of 1 cm, using the simultaneously obtained difference spectra in the visible range and their respective extinction coefficients to determine the scaling factor. A 1:1 molar relation of cytochrome c_1 and the [2Fe-2S] protein and of Q_i and cytochrome b_H was assumed.

IR difference spectra of the complex in ^2H_2O and of the ^{15}N-labeled complex were obtained in three redox regions: for cytochrome c_1 and the [2Fe-2S] protein for cytochrome b_H and Q_i and for cytochrome b_L. The experiments were done at pH/pD 6.5 and 8.7. Peak positions are given in Table 3. The spectra of the reduction of both cytochrome b_H and Q_i are shown in Figure 5. Details will be presented in the Discussion.

All infrared difference spectra show signals in the 1690−1610 cm^{-1} and in the 1575−1480 cm^{-1} spectral regions. The first region indicated includes the amide I absorbtions from the C═O stretch vibrations of the protein backbone. The signals are narrow in the spectra obtained for all cofactors except for Q_i. They are shifted by a few wavenumbers after $^1H/^2H$ exchange of the sample (data not shown). Amide I vibrations are reported to shift by 2−12 cm^{-1} depending on the secondary structure of the respective peptide backbones, with 2 cm^{-1} for α-helical structures (*30*). The amide I peak

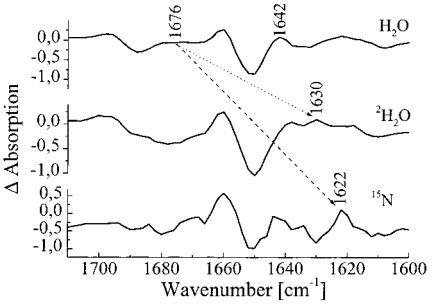

FIGURE 5: Reduced minus oxidized spectra of cytochrome b_H and the quinone bound to Q_i binding site as obtained at pH 6.5. (Top) pH 6.5; (middle) pD 6.5; (bottom) ^{15}N-labeled complex, pH 6.5.

in the absorption spectra of the cytochrome bc_1 complex (data not shown) is shifted by 2 cm^{-1} after $^1H/^2H$ exchange, reflecting the predominant α-helical structure of the complex. The 1575−1480 cm^{-1} spectral region includes the amide II signals, a coupled mode of the C−N stretch and N−H bending vibration of the protein backbone. However, contributions from quinone and heme modes and amino acid side-chain vibrations are also evident. Exchange of ^1H against ^2H uncouples the C−N and the N−D vibration, leading to a shift of the signals to around 1480 cm^{-1} for the C−N vibration (data not shown) and to wavenumbers smaller than 1000 cm^{-1} for the N−D vibration (*30*). ^{15}N exchange leads

to a shift of the amide II signals in the absorption spectra of the cytochrome bc_1 complex from 1546 to 1530 cm^{-1} (data not shown). Difference signals in the two spectral regions indicate changes of the geometry of the protein backbone, induced by the redox reactions of the cofactors.

The difference spectra of each heme and its protein environment show maxima at 1554 cm^{-1} and 1534 cm^{-1} (Figures 2a,c,d and 3a,b). They can be assigned to the C_aC_m and C_bC_b heme stretch vibrations of the hemes by comparison with spectra of model compounds (*31*, *32*). In the spectrum of cytochrome b_L the signal at 1554 cm^{-1} is overlapped by an amide II vibration. It appears at 1548 cm^{-1} after $^1H/^2H$ exchange, which results in a shift of the amide II signals (data not shown). The $C_\alpha N$ heme vibration of both cytochrome c_1 and cytochrome b_L are present at 1402 cm^{-1} as a maximum, while the C_mH heme vibration of the *b* hemes is at 1236 cm^{-1} and that of cytochrome c_1 is at 1240 cm^{-1} (assignments according to ref *31*). The $C_\alpha N$ vibration of the heme b_H might be overlapped by the symmetric COO^- stretch vibration of an aspartic or glutamic acid leading to the negative signal at 1402 cm^{-1} (see below). Contributions of heme vinyl vibrations of the *b* hemes could tentatively be assigned to the maxima at 1608 cm^{-1} ($C_\alpha C_\beta$) and to the minima at 1140 cm^{-1} ($C_\alpha C_\beta$ stretch) for cytochrome b_L and at 1102 cm^{-1} (CH_2 deformation) for cytochrome b_H (*31*, *32*). At 1608 cm^{-1}, however, contributions from amino acid side chains like glutamine, asparagine, histidine, tyrosine, and arginine potentially overlap the heme vinyl vibration, provided that the extinction coefficients are strong enough, which makes histidine the less probable candidate. At 1102 cm^{-1} a contribution of histidine signals cannot be excluded.

The IR difference spectra of the quinone (Figures 2e and 3c) show signals, which can be attributed to the quinone itself by comparison to spectra of ubiquinones and ubiquinols in solution (*33*). The negative and inhomogeneous signal at 1650 cm^{-1} at least partly can be attributed to the C═O stretching mode of the ubiquinone. The entire signal is shifted to higher wavenumbers at pH 6.5. A pH dependence of the IR signals of quinones is not expected on the basis of their IR spectra in different organic solvents such as MeOH, methanol, acetonitrile, and tetrahydrofuran (*33*). The pH-dependent part of the inhomogeneous signal is therefore attributed to an amide I signal overlapping the quinone C═O stretching mode. The minimum at 1608 cm^{-1} in our spectra is not affected by deuteration and therefore assigned to the C═C vibration of the quinone ring. The C−C vibration of the quinone (*34*, *35*) may correspond to the negative signals at 1284 and 1262 cm^{-1}. The latter was also attributed to the C−O vibration of the quinone (*35*). The signals at 1202 and 1150 cm^{-1} may also be caused by the methoxy group of the quinone (*36*−*39*). In our spectra all four signals are independent of pH and not shifted by deuteration or labeling of the complex with ^{15}N, thus confirming the attribution of the bands to vibrational modes of the quinone itself.

After reduction, three positive signals appear at 1464, 1428, and 1388 cm^{-1}. Positive signals in the 1500−1350 cm^{-1} spectral region are typical for the reduction of quinones (*33*, *40*, *41*). The maximum around 1428 cm^{-1}, which is independent from $^1H/^2H$ exchange and ^{15}N labeling and can be attributed to the aromatic C−C stretch vibration of the quinol (*33*). A clear identification of the C−O mode of the quinol is not possible at present. ^{13}C labeling of the quinone in the 1- and 4-positions will be necessary to attribute this mode. At 1464 cm^{-1} the $C-CH_2$ isoprenoid vibration and at 1388 cm^{-1} the $C-CH_3$ isoprenoid vibration can preliminarily be assigned (*35*). Contributions of the methyl or methoxy groups around 1464 cm^{-1} have been discussed as well (*42*). The small amplitudes of the three signals in our spectra compared to the amplitude of the negative signals of the C−C and C−O vibrations of the quinone support the assignment of the spectra to the quinol formation. Positive signals at 1468, 1429, and 1391 cm^{-1} were also observed after UV irradiation of UQ10 at 270 K and were assigned to nonradical photoproducts (*41*). By UV irradiation at 10 K the same authors could stabilize the semiquinone radical, and bands in the C−H bending region were described at 1473, 1415, and 1367 cm^{-1} (*41*). Their amplitude was observed to be about the size of the amplitude of the heme vinyl vibration at 1608 cm^{-1} (*40*, *41*). Position and amplitude of the signals in our spectra therefore justify the attribution of the spectrum to quinol formation. Furthermore, appearance and disappearance of a semiquinone intermediate during the course of the redox titration will not contribute to the amplitudes in the spectra of cytochrome b_H and Q_i as obtained by a fit of the titration data to a sum of two Nernst equations. We tested on simulated data sets that the program assigned the amplitude and average redox potential of the two electron quinone reaction to one Nernst equation for Q_i. At pH 6.5 the amplitude of all signals of the quinone spectrum is diminished by a factor of 2 with respect to the amplitude obtained at pH 8.7. We interpret this result by a difference in Q_i site occupancy of a factor of 2 (see below).

The spectra obtained at pH 8.7 in Tris-HCl buffer for cytochrome c_1, the [2Fe-2S] protein, Q_i, and cytochrome b_L (Figure 2a,b,d,e) show a minimum at about 1066 cm^{-1}: This signal can be assigned to the absorption of the protonated CNH_2 group of Tris-HCl buffer, which disappears due to proton release of the buffer by proton uptake of the protein during the reduction of the respective cofactors. At pH 6.5 in potassium phosphate buffer a maximum around 1086 cm^{-1} appears in all spectra. It can be assigned to the absorption of the deprotonated potassium phosphate buffer. It indicates a proton uptake of the protein due to the reduction of the cofactors. The difference spectra of cytochrome c_1 and the [2Fe-2S] protein could not be separated at this pH value because of their similar midpoint potentials. The protons involved in the redox reactions of these two cofactors at pH 6.5 may originate from one or from both of the two protein subunits. Table 4 summarizes the calculated number of protons picked up or released from the protein during the redox transition of each of its cofactors.

Denaturation Signals. Raising the redox potential applied to the bc_1 complex at pH 8.7 from +460 mV, where all cofactors are already oxidized, to higher values causes a spectrum with two broad maxima of high amplitude (Figure 6) at 1630 and 1522 cm^{-1}. The peak at 1522 cm^{-1} was not shifted in the ^{15}N labeled complex, excluding an assignment to an amide II vibration. Among other small signals at lower frequency a small maximum at 1562 cm^{-1} appears. Furthermore, a peak is observed at 2108 cm^{-1}. All these signals are not reversible if the potential of +460 mV is applied again. At pH 6.5 these signals were not observed, even if the potential was raised as high as +610 mV.

Table 4: Protonation Reactions of the bc_1 Complex[a]

	experimental values of this work				literature values			
compound	pH 6.5		pH 6.5		pK_{ox}	pK_{red}	pH 6.5	pH 8.7
cytochrome c_1	0.6 ± 0.4		0.5 ± 0.7	0.2	9	basic	0	0.3
[2Fe-2S] protein				0.5	8; 7.6, 9	>11	0	0.6; 0.8
cytochrome b_H	1.9 ± 1.2	0.6	1.9 ± 0.4	0	>6	7.7	0.8	0.1
quinone Q_i		1.2		1.9			2	2

[a] Proton uptake of the complex during the reduction of the different cofactors. The numbers in columns 3 and 5 are each calculated from one spectrum originating from a redox titration. The values in columns 2 and 4 are average values and standard deviations originating from 57 experiments (40 at pH 6.5 and 17 at pH 8.7). For references see text.

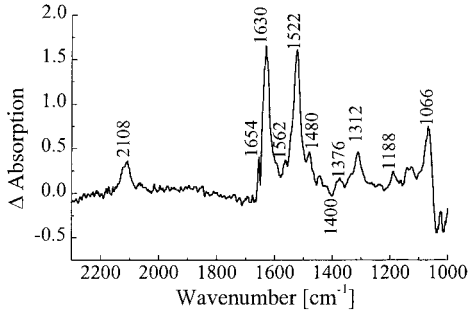

FIGURE 6: IR difference spectrum of the denaturation of the [2Fe-2S] protein. A spectrum recorded at +260 mV (all cofactors of the complex oxidized) has been subtracted from a spectrum recorded at +510 mV. The spectrum is normalized to a protein concentration of 1 mM and a path length of 1 cm.

DISCUSSION

Accessibility of Cofactors. The heme of cytochrome c_1 exhibits direct, fast, and reversible electrochemical redox reactions with the modified electrode, as does soluble cytochrome *c* (*21*). The addition of mediators is thus not necessary for the redox reaction of cytochrome c_1. This indicates that the heme is accessible from the external surface and therefore at an exposed position in the protein. These observations have recently been confirmed by the crystal structure, which shows that the pyrrole C comer of the heme c_1 is exposed to the protein surface (*16*).

The redox reaction of the [2Fe-2S] cluster in the absence of mediators could only be observed at pH 6.5. At pH 6.5, the midpoint potentials of the [2Fe-2S] protein and cytochrome c_1 are very close to each other, thus allowing cytochrome c_1 to act as a mediator between the electrode and the [2Fe-2S] protein. At pH 8.7, the difference in the midpoint potentials is about 60 mV. The poor overlap of the potential ranges for the redox reactions of these two cofactors allows the reduction of only a few percent of the [2Fe-2S] protein by cytochrome c_1.

The reaction of cytochrome b_H at pH 6.5 in the absence of mediators may be mediated by the quinone bound to the Q_i binding site. At pH 8.7, no reactions of the quinone or of cytochrome b_H without mediators were observed. The reason for this observation may be a change in the accessibility of the bound quinone at this pH value.

Midpoint Potentials. The use of IR spectroscopy has allowed the midpoint potential of the [2Fe-2S] protein in the bc_1 complex to be determined for the first time at physiological temperature. The values obtained, +337 mV at pH 6.5 and +288 mV at pH 8.7, are slightly above the range of literature values, which were mainly determined by EPR spectroscopy for the [2Fe-2S] cluster in the bc_1 complex to be between +274 and +308 mV at pH 7 (*4*, *6*, *20*, *28*, *29*, *43*, *44*) or by cyclic voltammetry for the isolated [2Fe-2S] subunit to be +310 and +240 mV at pH 6.5 and 8.7, respectively (*45*). They show a more pronounced pH-dependence than the values determined in our work. The two pK-values of 7.6 and 9 determined by Link (*46*) and Cocco et al. (*47*) for the oxidized state of the isolated [2Fe-2S] subunit of bovine mitochondria bc_1 complex do not agree with the pH dependence of the redox potentials of the [2Fe-2S] protein from *Rb. capsulatus* bc_1 complex. This reflects different properties of the two redox centers either because they are from two different species or because the isolation of the subunit from the complex changes its redox properties.

The midpoint potentials obtained in this work for the quinone occupying the Q_i site are +170 mV at pH 6.5 and +44 mV at pH 8.7. They are in very good agreement with the redox potentials published by Robertson et al. (*12*) and Ding et al. (*6*) for the quinone bound to the Q_i binding site (+48 mV at pH 8.7 and +180 mV at pH 6.5). These potentials and the two protons released during complete reduction of the quinone at pH 8.7 clearly allow us to assign the quinone reactions observed here exclusively to the quinone bound to the Q_i binding site.

Potentials of the *b* hemes correspond to the values observed for the same complex by chemical redox titration (*20*). Surprisingly, the midpoint potential of cytochrome c_1 was found to be a significant 50 mV more positive under the conditions of this work.

Extinction Coefficients of the Cytochromes in the Visible Spectral Range. While the reduced minus oxidized difference extinction coefficient of cytochrome b_H (21.9 mM^{-1} cm^{-1} at 561 nm − 575 nm) determined in this work is consistent with earlier works, the values for cytochrome c_1 (11.9 mM^{-1} cm^{-1} at 553 nm − 575 nm) and cytochrome b_L (6.7 mM cm^{-1} at 566 nm − 575 nm) are smaller than the values used so far of 20 mM^{-1} cm^{-1} (*48*) or 19.5 mM^{-1} cm^{-1} (*49*) for each of the cytochromes of the bc_1 complex or of 17.5 mM^{-1} cm^{-1} for cytochrome c_1 (*50*). The values for the cytochromes *b* are in reasonable agreement with the results of Dutton and Jackson (*51*), who observed an amplitude distribution of 29:14 for cytochrome b_H:b_L. In addition, the large half-width of the α-band of cytochrome b_L, originating from different electronic levels occupied in the exited state of the heme, may also account for its smaller amplitude.

The α-band of cytochrome c_1 has the smallest half-width of all cytochromes of the complex. An explanation for its small amplitude is thus not obvious. However, its redox reaction is fast and reversible, indicating that a complete reaction of the heme occurred in each measurement. In our

work it could be demonstrated that the small shoulder in the spectrum of cytochrome b_H is an intrinsic property of the subunit, similar to the well-known splitting of the α-band of cytochrome b_L.

IR Difference Spectra: (A) Amide Signals. The amide signals in the IR difference spectra indicate changes in the geometry of the protein backbone. They are sensitive to changes in the C−O dipole strength and therefore represent localized conformational changes rather than global rearrangements. The signals are narrow for the cytochromes and the [2Fe-2S] protein, showing well-defined, small conformational changes, originating from the redox transition of the cofactors. The amplitude of the amide I signals are on the same order of magnitude as those observed for cytochrome *c* (*21*) showing small conformational changes of the protein backbone during the redox transition of the cofactor, involving a few amino acids. Besides the protein signals, heme and quinone modes can absorb in this spectral region as discussed below. The spectrum of the [2Fe-2S] protein, in contrast, is a pure protein spectrum (Figure 2b). Because of the heavy masses of the sulfur and the iron atoms, their vibrations will occur at frequencies lower than 1000 cm^{-1}. The overall amplitude of the amide I signals of the [2Fe-2S] protein correspond to 1.3×10^{-3} absorption units (AU) in contrast to 0.8×10^{-3} and 0.9×10^{-3} absorption units for the cytochromes. Both signals, however, can be explained by two or three amino acids involved in a particular secondary structure, which is altered upon redox transition of the cofactor. Recently, the [2Fe-2S] protein has been crystallized in two conformations (*15*, *16*). Kim et al. (*52*) deduce from different electron densities in the presence or absence of inhibitors an influence of Q_o-site occupancy on the mobility of the [2Fe-2S] protein. Brugna et al. (*53*) investigated the orientation of the [2Fe-2S] protein in its oxidized and reduced state by EPR spectroscopy on partially ordered membranes. They concluded that the [2Fe-2S] protein moves during the reaction cycle of the complex from a position close to heme c_1 in its oxidized state to a position close to the Q_o binding site in its reduced state. It should be mentioned that the movement of the entire [2Fe-2S] subunit during the redox cycle of the protein by some 10 Å need not be represented by large signals in the amide I region. It is possible and in agreement with the structural data that the whole extramembraneous domain of the [2Fe-2S] protein does not change its structure during the movement. Only the conformation of a few backbone bonds working at the hinge region of the amino acid chain tether between the transmembrane helix and the extramembraneous domain may be changed, thus resulting in relatively small amide I signals as observed here. In contrast to the narrow and small signals of the [2Fe-2S] protein and the cytochromes, the quinone spectrum obtained at pH 8.7 (Figure 2e) shows signals of larger amplitude and half-width. These signals are composed in part by the quinone itself (see below) but also by a considerable contribution of amide signals. This is indicated by important band shifts in the amide II region after $^1H/^2H$ exchange, especially for the broad negative signal between 1540 and 1510 cm^{-1}. Moreover in the amide I region the broad maximum around 1620 cm^{-1} and the minima at 1680 and 1664 cm^{-1} can be assigned to protein backbone vibrational changes by their small shifts after $^1H/^2H$ exchange as well as probably part of the minimum at 1652 cm^{-1}, which is overlapped by a quinone band (see below). The large signals can be interpreted in terms of a rearrangement of the quinone-binding site during the redox reaction of the quinone, which changes the secondary structure of some amino acids. Furthermore, certain flexibility in the structure of the binding site can be deduced from the considerable half-width of the signals.

The signals observed in the spectrum obtained at pH 6.5 are of much smaller amplitude. The same scaling factor was used for the quinone spectra and the spectra of cytochrome b_H, assuming that one quinone is present in each Q_i binding site. This was the case at pH 8.7 (see below). The smaller amplitudes at pH 6.5 may reflect that only approximately half of the binding sites have been occupied at pH 6.5.

(B) Heme Signals. The signals at 1554 and 1534 cm^{-1} attributed to heme vibrations are more pronounced in amplitude in the spectra of cytochrome subunits of the cytochrome bc_1 complex and other heme containing protein complexes (tetraheme subunit of *Rhodopseudomonas viridis* and *Chloroflexus aurantiacus* (*54*)) than in the spectra of the soluble *c*-type cytochromes (*21*, *55*). They may indicate a more rigid protein environment of the heme-binding site in the protein complexes than in the small and soluble *c*-type cytochromes, forcing two different conformations of the porphyrin ring in its two redox states.

In the reduced minus oxidized difference spectrum of cytochrome *c*, a positive signal of large amplitude at 1690 cm^{-1} was tentatively assigned to the vibration of a protonated heme propionate in reduced cytochrome *c* (*21*). In the spectra of both *b* hemes a negative signal at 1690 cm^{-1} is present. If this signal should be interpreted as a heme propionate signal according to ref *21*, it would mean that protonation of the propionates during the oxidation of the hemes occurs. This, however, is highly improbable for reasons of electrostatic interaction energy. We therefore conclude that this signals are not due to protonated propionates but rather to amide I vibrations and that the heme propionates of bc_1 complex do not undergo proton exchange during their redox reactions.

(C) Amino Acid Side-Chain Signals. The absorption of amino acid side chains such as tyrosine, aspartic and glutamic acid, asparagine, glutamine, and arginine is intense enough to be detectable in IR difference spectra. Histidine, lysine, tryptophan, and proline show smaller extinction coefficients but they might be detectable in some cases as well. Vibrations of other amino acids side chains are not supposed to contribute to the IR signals in the spectral range investigated here. In most spectral regions side-chain signals are overlapped by signals of the protein backbone or the cofactors, making assignment difficult. An exception is the C═O stretch vibration of protonated aspartic and glutamic acid side chains, absorbing above 1700 cm^{-1}, where no other protein modes are expected. Such signals are seen in the spectra of the *b* cytochromes. The pH dependence of their amplitudes even allows us to assign the p*K* value of the absorbing group. A loss in the band above 1700 cm^{-1} upon deprotonation of the side chain should result in two bands at about 1620 and 1570 cm^{-1} (antisymmetric COO mode) and about 1450−1420 cm^{-1} (symmetric COO mode). However, these difference signals are much more difficult to detect due to multiple overlap by other difference signals of the protein and the cofactors.

Cytochrome b_L shows two signals at 1720 and 1704 cm^{-1} at pH 6.5 (Figure 3b). At pH 8.7 only one signal at 1720 cm^{-1} is present (Figure 2d); its amplitude is diminished to half the size of the corresponding signal at pH 6.5. The 1704 cm^{-1} signal is at the limit between a protonated carboxylic residue and a high-frequency amide I mode, as for example from a proline. The signal at 1720 cm^{-1}, however, is at a position where nothing other than a signal from a carboxylic group is expected for the present sample. Therefore a pK_s around 8.7 can be assigned to the group absorbing at 1720 cm^{-1}. Provided that further site-directed mutagenesis studies confirm our preliminary assignment of the 1704 cm^{-1} signal to a protonated carboxylic group, its pK_s is between 7 and 8. Both p*K* values seem unusually high for aspartic and glutamic acids, which show p*K* values around 4 in aqueous solution. However, a shift of the p*K* of aspartic and glutamic side chains to much higher values in proteins has been demonstrated. Recently proton coupling between a glutamic acid and the heme has been demonstrated for a four-helix bundle—a maquette for cytochrome *b* of the bc_1 complex (*56*). The structure of the bc_1 complex shows, that there are several conserved glutamic or aspartic acids in the 20 Å environment of cytochrome b_L (PDB ID code 3BCC). One conserved glutamic acid of the cytochrome c_1 subunit (Glu239) and an aspartic acid of the transmembrane helix of the [2Fe-2S] protein (Asp43), described as the first residue of the tether (*16*), are close to the heme b_L. They are located on the periplasmic site of the heme. Furthermore, two carboxylic residues of the *b*-subunit (Glu278 and Asp187) are in the vicinity of the heme. The first one is closest to the heme and just beside the conserved Asn279, which has been identified by mutagenesis to be part of the Q_o binding site (*5*). It therefore seems to be the most promising candidate for one of the discussed difference signals.

Cytochrome b_H at pH 6.5 also exhibits two signals in this spectral region at 1720 and 1702 cm^{-1}. Unfortunately, in the spectrum obtained at pH 8.7, the signal-to-noise ratio in this spectral region is not sufficient to clearly identify these signals. At pH 8.7, the spectrum of cytochrome b_H shows negative signals at 1574 and 1402 cm^{-1}, which are not present in the spectrum of cytochrome b_H obtained at pH 6.5. The antisymmetric and the symmetric stretching vibrations of the deprotonated carboxyl groups are expected at these positions. The presence of small signals at above 1700 cm^{-1} in combination with negative signals at 1574 and 1402 cm^{-1} may be taken as a hint to a possible deprotonation of an aspartic or glutamic acid induced by the oxidation of the heme b_H at pH 8.7.

Arginine vibrations can tentatively be assigned in the spectra of cytochrome *b*. The symmetric stretching vibration of arginines is expected at 1635 cm^{-1}, and the antisymmetric stretching vibration around 1670 cm^{-1} (*63*). The spectrum of cytochrome b_H shows two maxima at 1676 and at 1642 cm^{-1}. The signals appear as well in the spectra of Figure 4b, which show the redox-induced spectral changes of cytochrome b_H and the quinone Q_i before deconvolution into the difference spectra of the two compounds. Figure 5 shows the difference spectra of cytochrome b_H and the quinone Q_i in H_2O, ^2H_2O, and after ^{15}N exchange. After $^1H/^2H$ or ^{15}N exchange, the peaks are shifted. At pH 6.5 the maximum at 1676 cm^{-1} disappears and positive signals at 1634 and 1622 cm^{-1} appear after $^1H/^2H$ and ^{15}N exchange respectively (Figure 5). Chirgadze et al. (*64*) observed signals at 1608 and 1586 cm^{-1} on deuterated samples of isolated argnine. The protein environment may shift the band position observed from the model compound at 1608 cm^{-1} to the 1634 cm^{-1} observed here. ^{15}N exchange is expected to shift the signal by 50 cm^{-1} to lower wavenumbers, according to simplifying calculations for an isolated C−N stretch vibration. Indeed, a shift of 54 cm^{-1} is observed in our spectra.

Arginines have already been postulated to form salt bridges to the propionic acids of both *b* hemes (*2*). Furthermore, construction of model peptides for the environment of the *b* hemes showed that the guanidine group of arginine 114 influences the midpoint potential of the heme b_H (*65*). Recently the crystal structure showed, that the propionate of heme b_H adopted a twisted conformation in order to form an ion pair with the homologous arginine in the cytochrome bc_1 complex from chicken mitochondria (*16*).

The spectrum of the [2Fe-2S] protein shows signals at 1462 and 1446 cm^{-1}, a region where ring vibrations of proline and tryptophan absorb (*66*, *67*). Both signals are not influenced by $^1H/^2H$ exchange but shift in the spectra obtained from the ^{15}N-labeled bc_1 complex by a few wavenumbers as expected for proline or tryptophan ring vibrations. Two prolines are present in the vicinity of the [2Fe-2S] cluster (Pro170 and Pro154). Especially the conserved Pro154 is supposed to interact with the cluster, since mutation of this residue shifts the midpoint potential of the [2Fe-2S] cluster in yeast (*68*).

Protonation Reactions. It is well-known that oxidation−reduction reactions of a cofactor can induce p*K* shifts and proton exchange in adjacent acid/base amino acid side chains. One proton per electron charge can be released during cofactor oxidation if the p*K* shift of the amino acid side chain is sufficiently large and if the p*K* values of the amino acid side chain when exposed to the reduced or oxidized cofactor are situated well above and below the ambient pH value. A variety of chemical, physical, and environmental factors can affect the range and extent of the p*K* shift, and if the pH is outside the range of the p*K* shift or it is small, then the proton per electron charge ratio will fall from 1 to as low as 0.

A novel technique of proton measurement allowed us direct observation of the protein proton release and uptake in the IR spectral range by observation of the buffer modes. The number of protons picked up or released from the protein during the redox reaction of each cofactor was quantified by analysis of the IR modes of the buffer. Thus no addition of substances such as pH-indicating dyes is necessary and the buffer capacity can be chosen freely. The technique therefore is especially useful in cases of small sample volumes and high protein concentrations.

In Table 4 these values are compared to literature values as deduced from the p*K* values for the reduced and the oxidized states of the cofactors (*19*, *46*, *47*, *58*, *60*, *61*, *65*, *69*). Results show that there is less than one proton involved in redox reactions of cytochrome c_1, the [2Fe-2S] protein, and cytochrome b_H. For the two cytochromes and the [2Fe-2S] protein at pH 8.7, the values are in good agreement with literature values. The redox reactions of cytochrome b_L have been very slow under our experimental conditions and it was difficult to reach equilibrium. Protons released during the reduction of the heme could be observed, but their number could not be quantified.

Careful examination of the errors that might occur in the determination of the number of protons involved in the redox reactions of the complex included possible pH changes of the surrounding buffer due to proton release of the protein, the buffer capacity of the protein, and protonation reactions of the mediators.

The pH value of the buffer could be calculated to vary by no more than ±0.1 pH unit. To estimate the buffer capacity of the protein, p*K* values of side chains in aqueous solution were considered to be applicable to residues at the surface of the protein. There are histidine residues having p*K* values close to pH 6.5. The amino termini of the protein subunits and the thio group of the cysteine have p*K* values close to pH 8.7. There are only two cysteine residues in the sequence of cytochrome bc_1 complex that are not involved in ligation of cofactors or disufite bridges. The buffer capacity of these two residues and the three protein amino termini is negligible at pH 8.7. Twenty-one histidines are on the surface of the protein, and hence they are not part of transmembrane α-helices or acting as ligands. They can serve as buffer systems at pH 6.5. At a protein concentration of 2 mM (average concentration used in our experiments), 10 mM protons will be released during the reduction of all cofactors of the complex and cause a change in the pH value of the solution of 0.1 pH unit. Then 2 mM protons (i.e., one proton per complex) will be buffered by the histidine residues and therefore not be detectable via buffer signals. The IR signal of the protonated pyrimidine nitrogen is unfortunately too small to be detected in IR difference spectra.

Mediators have been present in a concentration of 40 μM in our experiments. A control experiment reveals that 1.6 mM protons are released during the complete reduction of all mediators. At the average protein concentration of 2 mM, 0.8 proton detected per bc_1 complex therefore will originate from the mediators and not from the protein. This effect and the buffer capacity of the protein are working in opposite directions, compensating at least partially their respective contributions.

We measured 0.6 proton released during the reduction of both the [2Fe-2S] cluster and cytochrome c_1 at pH 6.5. According to p*K* values determined by other authors for cytochrome c_1 (*70*), no protonation reactions are expected at this pH value for cytochrome c_1. If we therefore assign all protons observed to the [2Fe-2S] protein we propose a pK_{ox} less than 7 for this subunit. We can exclude that aspartic or glutamic acids are involved in the protonation reactions associated with the redox reactions of the [2Fe-2S] protein, because of the lack of IR signals in the difference spectra at frequencies above 1700 cm^{-1}.

For cytochrome b_H we measured 0.6 proton at pH 6.5 and no protonation reactions at pH 8.7. This is close to literature values (*58*−*62*). Protonation reactions of cytochrome b_L could be detected at both pH values, consistent with no p*K* value in this region (see ref *59*), suggesting that the redox reactions of the heme b_L are pH-dependent over the whole range of pH values investigated here. IR difference spectra of the *b* hemes reveal that the protonatable group responsible for the pH dependence of the midpoint potentials and the protonation reactions observed by buffer signals might be an aspartic or glutamic acid, as discussed above. As already mentioned, amplitude of the quinone spectra were calculated by assuming one quinone per Q_i binding site. This assumption is correct in the case of measurements made at pH 8.7, as can be seen from the two protons involved in the redox reaction of the quinone. At pH 6.5, however, the number of protons calculated and amplitudes in the infrared difference spectra are approximately half the size as the values obtained at pH 8.7. We therefore conclude that at pH 6.5 occupancy of the Q_i binding site is around 50%.

Denaturation Reactions. The spectrum of the irreversible reaction obtained at high potentials at pH 8.7 (Figure 6) could be attributed to a further reaction of the already oxidized [2Fe-2S] protein by comparison with very similar spectra obtained for the isolated [2Fe-2S] subunit from bovine heart mitochondrial cytochrome bc_1 complex (data not shown). Denaturation may occur by oxidation of the deprotonated histidine ligands, which is followed by loss of the cluster. The big amplitude at 1630 cm^{-1} indicates structural changes of the protein backbone. We do not have an interpretation for the signals at 1522 and 2108 cm^{-1}. The 2108 cm^{-1} band is at a position where cyanide vibrations are expected. A complex between cyanide (from the mediator ferricyanide of the sample) with a small part of the bc_1 complexes might cause such a signal. However, the amplitude of the 2108 cm^{-1} signal measured here is 5−10 times bigger than the amplitude expected from cyanide, which was 50-fold less concentrated than the protein in our samples. The signal pattern of the two IR difference spectra from the [2Fe-2S] protein of *Rb. capsulatus* and bovine cytochrome bc_1 complex is identical with the exception of the positive signal at 1562 cm^{-1} in the spectrum of *Rb. capsulatus* bc_1 complex, which is at 1574 cm^{-1} in the spectrum of the isolated [2Fe-2S] subunit from bovine mitochondria. The former can be tentatively assigned to a glutamic acid, the latter to an aspartic acid. It is interestingly to note that, in the [2Fe-2S] protein discussed here, three of the conserved aspartic acids (Asp107, Aspl90, and Asp123 of bovine bc_1 complex) are replaced by glutamic acid residues (Glu83, Glu185, and Glu99 of *Rb. capsulatus* bc_1 complex). Glu99 has already been shown to be important in stabilizing the structure of the complex (*71*). The positive bands observed in the denaturation spectra are close to those observed for free Asp and Glu in aqueous solution (*63*), which may indicate that after denaturation the residues are exposed to water. The IR signals, furthermore, indicate proton release from the protein during its denaturation.

CONCLUSION

The present work represents the first study of a cytochrome bc_1 complex by redox-induced FTIR difference spectroscopy. Some assignments of vibrational modes observed in the spectra to redox-induced structural changes of the complex were proposed. Site-directed mutants and site-directed labeling of cofactors will be necessary to confirm our interpretations and to allow further assignments. Evaluation of the buffer modes to quantify protonation reactions of the protein has been proven to be a novel and promising application of infrared spectroscopy.

We are grateful to S. Grzybek for adaptation of the computer program ME_h-fit. We thank C. Berthomieu and A. Barth for careful reading of the manuscript and T. Link for providing the isolated [2Fe-2S] subunit of bovine heart mitochondria.

REFERENCES

1. Capaldi, R. A. (1982) *Biochim. Biophys. Acta 644*, 291−306.
2. Widger, W. R., Cramer, W. A., Herrmann, R. G., and Trebst, A. (1984) *Proc. Natl. Acad. Sci. U.S.A. 81*, 674−678.
3. Stonehurner, J., O'Brien, P., Green, C., Millet, F., Steidl, J., Yu, L., and Yu, C. A. (1985) *J. Biol. Chem. 259*, 5392−5398.
4. Robertson, D. E., and Dutton, P. L. (1988) *Biochim. Biophys. Acta 935*, 273−291.
5. Crofts, A. R., Hacker, B., Barquera, B., Yun, C. H., and Gennis, R. B. (1992) *Biochim. Biophys. Acta 1101*, 162−165.
6. Ding, H., Robertson, D. E., Daldal, F., and Dutton, P. L. (1992) *Biochemistry 31*, 3144−3158.
7. Meinhardt, S. W., and Ohnishi, T. (1992) *Biochim. Biophys. Acta 1100*, 67−74.
8. Gennis, R. B., Barquera, B., Hacker, B., Vandoren, S. R., Arnaud, S., Crofts, A. R., Davidson, E., Gray, K. A., and Daldal, F. (1993) *J. Bioenerg. Biomembr. 25*, 195−209.
9. Nakai, M., Endo, T., Hase, T., Tanaka, Y., Trumpower, B. L., Ishiwatari, H., Asada, A., Bogaki, M., and Matsubara, H. (1993) *J. Biol. Chem. 114*, 919−925.
10. Semenov, A. Y. (1993) *FEBS Lett. 321*, 1−5.
11. Degli Esposti, M., de Vries, S., Crimi, M., Ghelli, A., Patarnello, T., and Meyer, A. (1993) *Biochim. Biophys. Acta 1143*, 243−271.
12. Robertson, D. E., Prince, R. C., Bowyer, J. R., Matsuura, K., Dutton, P. L., and Ohnishi, T. (1984) *J. Biol. Chem. 254*, 1758−1763.
13. Brandt, U., and Trumpower, B. (1994) *Crit. Rev. Biochem. Mol. Biol. 29*, 165−197.
14. Ding, H., Moser, C. C., Robertson, D. E., Tokito, M. K., Daldal, F., and Dutton, P. L. (1995) *Biochemistry 34*, 15979−15996.
15. Xia, D., Yu, C.-A., Kim, H., Xia, J.-Z., Kachurin, M., Zhang, L., Yu, L., and Deisenhofer, J. (1997) *Science 277*, 60−66.
16. Zhang, Z., Hung, L., Shulmeister, V. M., Chi, Y.-I., Kim, K. K., Hung, L.-W., Crofts, A. R., Berry, E. A., and Kim, S.-H. (1998) *Nature 392*, 677−684.
17. Brasseur, G., Saribas, S. S., and Daldal, F. (1996) *Biochim. Biophys. Acta 1275*, 61−69.
18. Mitchell, P. (1975) *FEBS Lett. 59*, 137−139.
19. Rich, P. R. (1984) *Biochim. Biophys. Acta 768*, 53−79.
20. Robertson, D. E., Ding, H., Chelminski, P. R., Slaughter, C., Hsu, J., Moomaco, C., Tokito, M., Daldal, F., and Dutton, P. L. (1993) *Biochemistry 32*, 1310−1317.
21. Moss, D. A., Nabedryk, E., Breton, J., and Mäntele, W. (1990) *Eur. J. Biochem. 187*, 565−572.
22. Ljungdahl, P. O., Pennoyer, J. D., Robertson, D. E., and Trumpower, B. L. (1987) *Biochim. Biophys. Acta 891*, 227−241.
23. Baymann, F., Moss, D. A., and Mäntele, W. (1991) *Anal. Biochem. 199*, 269−274.
24. Grzybek, S., Baymann, F., Müller, K.-H., and Mäntele, W. (1993) in *Fifth international conference on the spectroscopy of biological molecules* (Theophanides, T., Anastassopoulou, J., and Fotopoulos, N., Eds.) pp 25−26, Kluwer Academic Publishers, Dordrecht, The Netherlands.
25. Yu, C. A., Yu, L., and King, T. E. (1974) *J. Biol. Chem. 249*, 4905−4910.
26. Iba, K., Takamiya, K.-I., and Arata, H. (1985) *FEBS Lett. 183*, 151−154.
27. Crofts, A. R., and Wraight, C. A. (1983) *Biochim. Biophys. Acta 726*, 149−185.
28. de Vries, S., Albrecht, S. P. J., Borden, J. A., and Slater, E. C. (1982) *Biochim. Biophys. Acta 681*, 41−53.
29. Prince, R. C., Lindsay, J. G., and Dutton, P. L. (1975) *FEBS Lett. 51*, 108−111.
30. Haris, P. I., and Chapman, D. (1994) in *Methods in Molecular Biology* (Mulloy, J. B., and Thomas, A. H., Eds.) Human Press Inc., Totowa, NJ.
31. Berthomieu, C., Boussac, A., Mäntele, W., Breton, J., and Nabedryk, E. (1992) *Biochemistry 31*, 11460−11471.
32. Choi, S., Spiro, T. G., Langry, K. C., Smith, K. M., Budd, D. L., and La Mar, G. N. (1982) *J. Am. Chem. Soc. 104*, 4345−4357.
33. Bauscher, M., and Mäntele, W. (1992) *J. Phys. Chem. 96*, 11101−11108.
34. Bellamy, L. J. (1968) *Advances in infrared group frequencies*, 3rd ed., Chapman & Hall, London.
35. Pennock, J. F. (1965) in *Biochemistry of quinones* (Morton, R. A., Ed.) pp 67−147, Academic Press, New York.
36. Isler, O., Rüegg, R., and Langemann, A. (1960) *Chem. Weekbl. 56*, 613−621.
37. Linn, B. O., Trenner, N. R., Shunk, C. H., and Folkers, K. (1959) *J. Am. Chem. Soc. 81*, 1263−1263.
38. Linn, B. O., Trenner, N. R., Arison, B. H., Weston, R. G., Shunk, C. H., and Folkers, K. (1960) *J. Am. Chem. Soc. 82*, 1647−1651.
39. Shunk, C. H., Wolf, D. E., McPherson, J. F., Linn, B. O., and Folkers, K. (1960) *J. Am. Chem. Soc. 82*, 5914−5918.
40. Breton, J., Thibodeau, D. L., Berthomieu, C., Maentele, W., Verméglio, A., and Nabedryk, E. (1991) *FEBS Lett. 278*, 257−260.
41. Burie, J. R., Boussac, A., Boullais, C., Berger, G., Matioli, T., Mioskowski, C., and Nabedryk, E. (1995) *J. Phys. Chem. 99*, 4059−4070.
42. Flaig, W. R., and Salfield, J. C. (1959) *J. C. Ann. Chem. 626*, 215−224.
43. Bowyer, J. R., Dutton, P. L., Prince, R. C., and Crofts, A. R. (1980) *Biochim. Biophys. Acta 592*, 445−460.
44. Matsuura, K., Bowyer, J. R., Ohnishi, T., and Dutton, P. L. (1982) *J. Biol. Chem. 258*, 1571−1579.
45. Link, T. A., Hagen, W. R., Pierik, A. J., Assmann, C., and von Jagow, G. (1992) *Eur. J. Biochem. 208*, 685−691.
46. Link, T. A. (1994) *Biochim. Biophys. Acta 1185*, 81−84.
47. Cocco, T., Lorusso, M., Dipaola, M., Minuto, M., and Papa, S. (1992) *Eur. J. Biochem. 209*, 475−481.
48. West, J. C., Mitchell, P., and Rich, P. R. (1988) *Biochim. Biophys. Acta 933*, 35−41.
49. Garcia, A. F., Venturoli, G., Gad'on, N., Fernandez-Velasco, J. G., Melandri, S. A., and Drews, G. (1987) *Biochim. Biophys. Acta 890*, 335−345.
50. Kohnishi, K., Van Doren, S. R., Kramer, D. M., Crofts, A. R., and Gennis, R. B. (1991) *J. Biol. Chem. 266*, 14270−14276.
51. Dutton, P. L., and Jackson, J. B. (1972) *Eur. J. Biochem. 30*, 495−510.
52. Kim, H., Xia, D., Yu, C. A., Xia, J. Z., Kachurin, A. M., Zhang, L., Yu, L., and Deisenhofer, J. (1998) *Proc. Natl. Acad. Sci. U.S.A. 95*, 8026−8033.
53. Brugna, M., S., Sinnig, I., and Nitsckke,W. (1999) *Proc. Natl. Acad. Sci. U.S.A.* (submitted for publication).
54. Fritz, F. (1995) Thesis, Albert-Ludwigs-University, Freiburg, Germany.
55. Baymann, F. (1991) DiplomArbeit, Univertät Freiburg, Germany.
56. Shifmian, M. J., Moser, C. C., Kalsbeck, W. A., Bociam, D. F., and Dutton, P. L. (1998) *Biochemistry 37*, 16815−16827.
57. Hacker, B., Barquera, B., Crofts, A. R., and Gennis, R. B. (1993) *Biochemistry 32*, 4403−4410.
58. Rich, P. R., Jeal, A. E., Madgewick, S. A., and Moody, A. J. (1990) *Biochim. Biophys. Acta 1018*, 29−40.
59. Petty, K. M., and Dutton, P. L. (1976) *Arch. Biochem. Biophys 172*, 346−353.
60. Semenov, A. Y., Bloch, D. A., Crofts, A. R., Drachev, L. A., Gennis, R. B., Mulkidjanian, A. Y., and Yun, C. H. (1992) *Biochim. Biophys. Acta 1101*, 166−167.
61. von Jagow, G., Link, T. A., and Ohnishi, T. (1986) *Biomembranes 18*, 157−180.
62. Gray, K. A., Robertson, D. E., Daldal, F., and Dutton, P. L. (1999) manuscript in preparation.
63. Venjaminov, S. Y., and Kalnin, N. N. (1990) *Biopolymers 30*, 1243−1257.
64. Chirgadze, Y. N., Fedorov, O. V., and Trushina, N. P. (1975) *Biopolymers 14*, 679−694.
65. Robertson, D. E., Farid, R. S., Moser, C. C., Urbauer, J. L., Mulholland, S. E., Pidikiti, R., Lear, J. D., Wand, A. J., Degrado, W. F., and Dutton, P. L. (1994) *Nature 368*, 425−431.

66. Rothshild, K. J., He, J., Gray, P., Roepe, P. D., Pelletier, S. L., Brown, R. S., and Herzfeld, J. (1989) *Proc. Natl. Acad. Sci. U.S.A. 86*, 9832−9835.
67. Fabian, H., Schultz, C., Backmann, J., Hahn, U., Saenger, W., Mantsch, H. H., and Naumann, D. (1994) *Biochemistry 33*, 10725−10730.
68. Gatti, D. L., Meinhardt, S. W., Ohnishi, T., and Tzagoloff, A. (1989) *J. Mol. Biol. 205*, 421−435.
69. Prince, R. C., and Dutton, P. L. (1976) *FEBS Lett. 65*, 117−119.
70. Prince, R. C., and Dutton, P. L. (1977) *Biochim. Biophys. Acta 459*, 573−577.
71. Graham, L. A., Brandt, U., Sargent, J. S., and Trumpower, B. L. (1993) *J. Bioenerg. Biomembr. 25*, 245−257.

BI990565B